

First Radical Cation Salt of Paramagnetic Transition Metal Complex Containing TTF as Ligand, $[\text{Cu}^{\text{II}}(\text{hfac})_2(\text{TTF-py})_2](\text{PF}_6) \cdot 2\text{CH}_2\text{Cl}_2$ (hfac = Hexafluoroacetylacetonate and TTF-py = 4-(2-Tetrathiafulvalenyl-ethenyl)pyridine)

Fatima Setifi,[†] Lahcène Ouahab,^{*,†} Stéphane Golhen,[†] Yukihiro Yoshida,[‡] and Gunzi Saito[‡]

Laboratoire de Chimie du Solide et Inorganique Moléculaire, UMR 6511 CNRS-Université de Rennes 1, Institut de Chimie de Rennes, Campus Beaulieu, F-35042 Rennes Cedex, France, and Division of Chemistry, Graduate School of Science, Kyoto University, Kyoto 606-8502, Japan

Received November 25, 2002

The preparation, X-ray crystal structure, EPR data, and magnetic measurement of $[\text{Cu}^{\text{II}}(\text{hfac})_2(\text{TTF-py})_2](\text{PF}_6) \cdot 2\text{CH}_2\text{Cl}_2$, a novel material where the conducting and the localized spin systems are covalently linked through conjugated bridges, are reported. The partial oxidation of the TTF-type organic donor ligand yielded the first radical cation salt of a paramagnetic transition metal complex. Moreover, this compound shows a mixed valence state at the unimolecular level, and additionally, the arrangement of the molecules in the crystal structure revealed the presence of isolated mixed valence TTF dimers.

Charge transfer salts of organochalcogenide electron donors have been subject of intense investigations and led to synthesis and physical characterization of a large number of materials with unusual electrical and magnetic properties.¹ In light of both applications to devices and fundamental science, recent interests are devoted to multifunctional molecular materials. In particular, materials based on the synergy between electrical conductivity and magnetic interactions are currently a subject of extensive studies in order to design long-range magnetic coupling between localized spins through the mobile electrons of the conducting networks (π -electrons).^{2–11} Up to now, works have been concerned mostly with salts composed of organic radical ions

containing mobile electrons and counterions having localized spins. Then, in these salts, the interaction could occur only through space, and therefore, it should be weak. We are investigating materials where the conducting and magnetic systems are covalently linked through a delocalized bridge which might enable magnetic exchange interactions between the localized spins and the mobile electrons. We reported recently new molecular building blocks, namely $\text{M}(\text{hfac})_2(\text{TTF-py})_2$ ($\text{M} = \text{Cu}^{\text{II}}, \text{Mn}^{\text{II}}$; hfac = hexafluoroacetylacetonate; TTF-py = 4-(2-tetrathiafulvalenyl-ethenyl)pyridine) where the ligand TTF-py is coordinated to a paramagnetic transition metal.^{10,11} Now we passed a new and very important step in the realization of the π -d system by the synthesis and characterization of the first radical cation salt of these coordination complexes. We report here the synthesis, X-ray crystal structure, and magnetic properties of $[\text{Cu}^{\text{II}}(\text{hfac})_2(\text{TTF-py})_2][\text{PF}_6]$.

The X-ray data were collected at 120 K from a single crystal.¹² The asymmetric unit contains one $[\text{Cu}^{\text{II}}(\text{hfac})_2(\text{TTF-py})_2]^{\text{+}}$ radical cation and one $[\text{PF}_6]^-$ anion both in special positions, (0,0,0) and (0,0,¹/₂), respectively, as well as one

* To whom correspondence should be addressed. E-mail: ouahab@univ-rennes1.fr.

[†] Institut de Chimie de Rennes.

[‡] Kyoto University.

- (1) (a) Williams, J. M.; Ferraro, J. R.; Thorn, R. J.; Carlson, K. D.; Geiser, U.; Wang, H. H.; Kini, A. M.; Whangbo, M. H. *Organic Superconductors. Synthesis, Structure, Properties and Theory*; Grimes, R. N., Ed.; Prentice Hall: Englewood Cliffs, NJ, 1992. (b) Ishiguro, T.; Yamaji, K.; Saito, G. *Organic Superconductors*; 2nd ed.; Springer, Berlin, 1998.
- (2) (a) Graham, A. W.; Kurmoo, M.; Day, P. *J. Chem. Soc., Chem. Commun.* **1995**, 2061. (b) Kobayashi, H.; Tomita, H.; Naito, T.; Kobayashi, A.; Sakai, F.; Watanabe, T.; Cassoux, P. *J. Am. Chem. Soc.* **1996**, *118*, 368. (c) Kobayashi, H.; Kobayashi, A.; Cassoux, P. *Chem. Soc. Rev.* **2000**, *29*, 325.

- (3) Nishijo, J.; Ogura, E.; Yamaura, J. I.; Miyazaki, A.; Enoki, T.; Takano, T.; Kuwatani, Y.; Iyoda, M. *Solid State Commun.* **2000**, *116*, 661. (b) Thoyon, D.; Okabe, K.; Imakubo, T.; Golhen, S.; Miyazaki, A.; Enoki, E.; Ouahab, L. *Mol. Cryst. Liq. Cryst.* **2002**, *376*, 25–32.
- (4) Coronado, E.; Galan-Mascaros, J. R.; Gomez-García, C. J.; Laukhin, V. N. *Nature* **2000**, *408*, 447.
- (5) (a) Turner, S. S.; Michaut, C.; Durot, S.; Day, P.; Gelbrich, T.; Hursthouse, M. B. *J. Chem. Soc., Dalton Trans.* **2000**, 905. (b) Setifi, F.; Golhen, S.; Ouahab, L.; Turner, S. S.; Day, P. *CrystEngComm* **2002**, *1*.
- (6) Sugawara, T. *Mol. Cryst. Liq. Cryst.* **1999**, *334*, 257.
- (7) Le Maguerès, P.; Ouahab, L.; Conan, N.; Gomez-García, C. J.; Delhaès, P.; Even, J.; Bertault, M. *Solid State Commun.* **1996**, *97/1*, 27.
- (8) Setifi, F.; Golhen, S.; Ouahab, L.; Miyazaki, A.; Okabe, K.; Enoki, T.; Toita, T.; Yamada, J. *Inorg. Chem.* **2002**, *41*, 3786.
- (9) Ouahab, L. *Chem. Mater.* **1997**, *9*, 1909.
- (10) Iwahori, F.; Golhen, S.; Ouahab, L.; Carlier, R.; Sutter, J. P. *Inorg. Chem.* **2001**, *40*, 6541.
- (11) Ouahab L.; Iwahori F.; Golhen S.; Carlier R.; Sutter J.-P. *Synth. Met.*, in press.

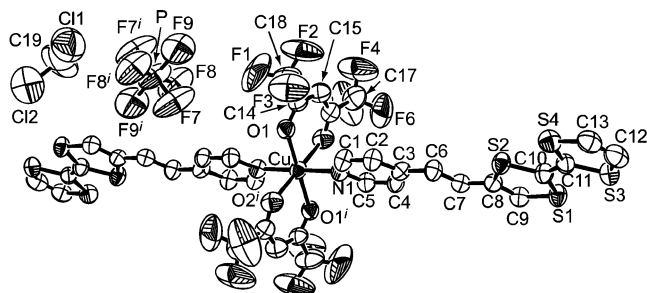


Figure 1. Molecular structure of $[\text{Cu}^{\text{II}}(\text{hfac})_2(\text{TTF-py})_2][\text{PF}_6] \cdot 2\text{CH}_2\text{Cl}_2$ with labeling scheme.

dichloromethane solvent molecule in general position. As usually observed for hfac ligand and PF_6 anion, large thermal coefficients together with residual peaks are found for the fluorine atoms suggesting high thermal motion and/or positional disorder for these atoms. In the molecular structure (Figure 1), the Cu atom is in a distorted octahedral coordination. It is bonded in the equatorial plane to two bidentate hfac anions through their oxygen atoms.

Two hfac anions are crystallographically equivalent, and Cu–O bond lengths are 1.999(4) and 2.290(5) Å, for Cu–O1 and Cu–O2, respectively. The TTF-py ligands occupy the apical positions and are *trans* to each other and bonded to the metal atom through the nitrogen atoms of the pyridyl ring with Cu–N bond length of 2.016(5) Å. The bond lengths around the Cu atom are very close to those found in the neutral complex; the central C–C bond length value of the TTF-py moiety (1.369(8) Å) which is more sensitive to oxidation is slightly larger than that found in the neutral complex (1.317(10) Å).¹⁰ From the stoichiometry, the following charge distribution might be deduced as $[\text{Cu}^{2+}(\text{hfac})_2^{2-}(\text{TTF-py})_2^{+}][\text{PF}_6]^-$ giving rise to mixed valence state in the unimolecular $[\text{Cu}^{2+}(\text{hfac})_2^{2-}(\text{TTF-py})_2^{+}]$ radical unit. In the crystal structure (Figure 2a), the TTF units form dimers separated by the PF_6 anions. The isolated dimers are of course in the mixed valence state.

The shortest intradimer S...S contact S1–S4 = 3.593(3) Å is in the van der Waals range. The TTF dimers and metal centers are connected by the delocalized pyridine bridge giving rise to linear chains parallel to the [1, 1, –1] direction.

EPR spectra were recorded down to 4 K with a JEOL JES-TE200 X-band ESR spectrometer equipped with a JEOL ES-CT470 cryostat. At 4 K, the EPR spectrum of powdered $[\text{Cu}(\text{hfac})_2(\text{TTF-py})_2][\text{PF}_6] \cdot 2\text{CH}_2\text{Cl}_2$ shows signals with anisotropic *g*-values ($g_{\parallel} = 2.324$ and $g_{\perp} \sim 2.0$, Figure 3) typical of a tetragonally elongated octahedral geometry.¹³ It is thus evident that the orbital ground state is the $(d_{x^2-y^2})^1$ orbital singlet and the d-spin interacts weakly with the two TTF-py

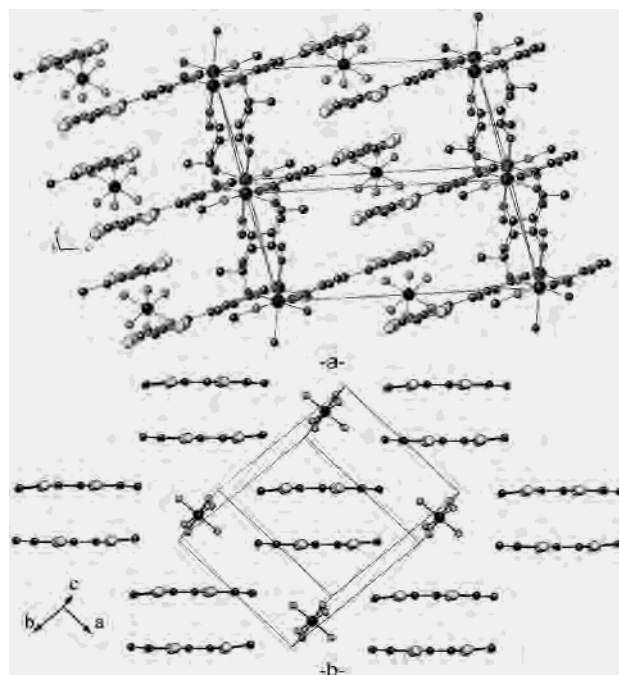


Figure 2. (a) Structure of the title compound, showing alternate organic/inorganic structure with the PF_6 anions incorporated in TTF layer; solvent molecules are omitted for clarity. (b) Projection in the *ab* plane showing the separation of the TTF dimers by the PF_6 anions.

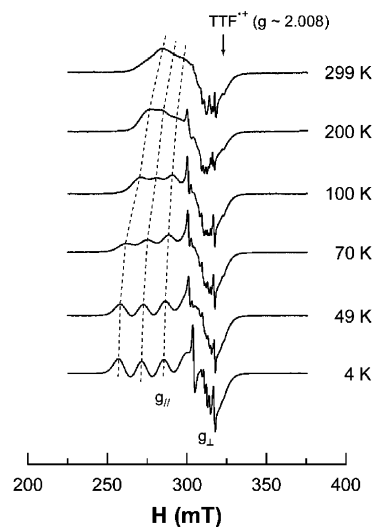


Figure 3. EPR spectra of powdered $[\text{Cu}(\text{hfac})_2(\text{TTF-py})_2][\text{PF}_6] \cdot 2\text{CH}_2\text{Cl}_2$ at typical temperatures.

moieties on the *z*-axis through the spin–orbit coupling. Hyperfine structure (coupling constant $A_{\parallel} = 134 \times 10^{-4} \text{ cm}^{-1}$) owing to coupling with the copper nuclear spin $I = 3/2$ splits the resonance into four signals. Signal confirming TTF-py^{•+} spins which clearly appear at $g = 2.008$ ¹⁴ in the 10^{-3} M acetonitrile solution is hardly observable for the powdered sample. The A_{\parallel} and g_{\parallel} values remain invariant up to 70 K, where they then begin to reduce more rapidly on increasing temperature, and attain to $A_{\parallel} = 94.3 \times 10^{-4} \text{ cm}^{-1}$

(12) Crystal data for $[\text{Cu}^{\text{II}}(\text{hfac})_2(\text{TTF-py})_2][\text{PF}_6]$: black parallelepipedic single crystal, Enraf-Nonius 4 circle diffractometer equipped with a CCD camera and a graphite-monochromated Mo K α radiation source ($\lambda = 0.71073 \text{ \AA}$); triclinic, space group $P1$ (No. 2), $M = 1409.40$, $a = 9.6998(5) \text{ \AA}$, $b = 10.2050(5) \text{ \AA}$, $c = 14.4317(10) \text{ \AA}$, $\alpha = 105.695(2)^\circ$, $\beta = 91.419(2)^\circ$, $\gamma = 97.719(2)^\circ$, $V = 1360.0(1) \text{ \AA}^3$, $Z = 1$; $D_c = 1.721 \text{ g cm}^{-3}$; $T = 120 \text{ K}$, $R = 0.0819$ for 3245 reflections with $I > 2\sigma(I)$; the structure was solved with SHELXS-97 and refined on F^2 with SHELXL-97 programs by full-matrix least-squares method.

(13) Abragam, A.; Bleaney, B. *Electron Paramagnetic Resonance of Transition Ions*; Clarendon Press: Oxford, 1970.

(14) Scott, J. S. In *Highly Conducting Quasi-One-Dimensional Organic Crystals*; Conwell, E., Ed.; Semiconductors and Semimetals, Vol. 27; Academic Press: New York, 1988; pp 385–436.

(15) Torrance, J. B.; Scott, B. A.; Welber, B.; Kaufman, F. B.; Seiden, P. E. *Phys. Rev. B* **1979**, *19*, 730.

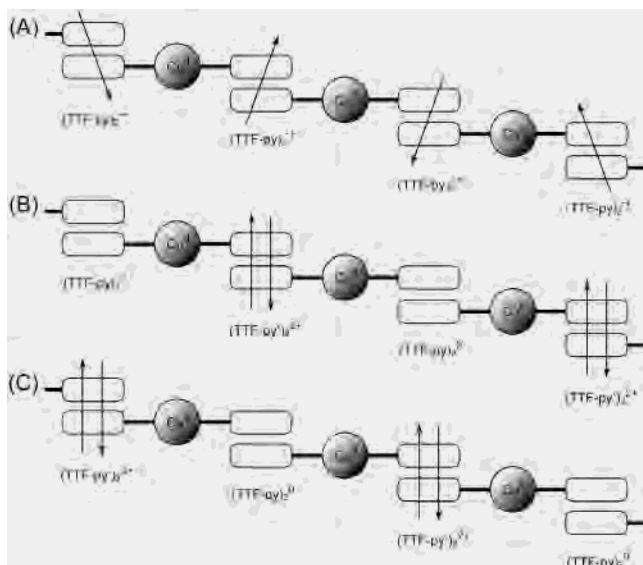


Figure 4. Schematic crystal structure of $[\text{Cu}(\text{hfac})_2(\text{TTF-py})_2][\text{PF}_6] \cdot 2\text{CH}_2\text{Cl}_2$ for the (A) equally charged state and (B, C) charge disproportionated state. Hfac parts are omitted. A vertical arrow indicates an unpaired spin for a TTF-py part.

and $g_{\parallel} = 2.265$ at 100 K. Along with the nearly isotropic spectrum with a g -value of about 2.15 at room temperature, these features are attributed to the dynamic Jahn–Teller distortion¹³ above 70 K.

A Quantum Design MPMS-XL SQUID magnetometer was used to collect static susceptibility data. Between 1.9 and 300 K, the magnetic susceptibility χ of $[\text{Cu}(\text{hfac})_2(\text{TTF-py})_2][\text{PF}_6] \cdot 2\text{CH}_2\text{Cl}_2$ can be fitted by the Curie–Weiss expression, $\chi \propto (T - \theta)^{-1}$, with Weiss temperature $\theta = -3.8$ K. The room-temperature effective moment μ_{eff} is $1.84(3) \mu_{\text{B}}$, which is much less than the value of $2.45 \mu_{\text{B}}$ expected from an uncorrelated two $S = 1/2$ spins composed of Cu^{II} and $(\text{TTF-py})_2^{+\bullet}$ spins. The observed μ_{eff} value also exceeds the value of $1.73 \mu_{\text{B}}$ expected for an independent $g = 2$, $S = 1/2$ system and reflects an increased g value of 2.1 estimated from the EPR spectrum at low temperatures, $g = (g_{\parallel} + 2g_{\perp})/3$. This result is essentially identical to what is proposed on the basis of the solid-state EPR spectra, in which only Cu^{II} spins with $S = 1/2$ spin were observable. The most probable reason for the absence of $(\text{TTF-py})_2^{+\bullet}$ spins is the charge disproportionation on TTF-py dimers (Figure 4B or C) instead of the equally charged state (Figure 4A). The electrical conductivity measured on compressed pellet is $\sigma_{\text{RT}} = 10^{-9} \text{ S} \cdot \text{cm}^{-1}$. UV–Vis–NIR spectra were measured in KBr pellets (2600–240 nm) on a Shimadzu UV-3100 spectrophotometer. In this case, the observed low-energy optical absorption band at around $5 \times 10^3 \text{ cm}^{-1}$ is readily assigned to the intramolecular transition from TTF-py^0 to $\text{TTF-py}^{+\bullet}$.¹⁵ However, the proposed spin state with two TTF-py dimers in a repeating unit seems to be in conflict with the structural refinement, which suggests crystallographically equivalent TTF-py dimers in the crystal. It is thus probable that the formation of the domain structures composed of those in Figure 4B,C prevents the diffraction pattern ascribable to the doubled periodicity.

Further work, particularly on the check on the diffuse spots, is in progress.

In conclusion, we demonstrated the possibility of partial oxidation of the TTF-type organic donor ligand yielding the first radical cation salt of a paramagnetic transition metal complex. In this novel material, the conducting and the localized spin systems are covalently linked through conjugated bridges. Moreover, this compound presented a mixed valence state at the unimolecular level, and additionally, the arrangement of the molecules in the crystal structure revealed the presence of isolated mixed valence TTF dimers. The interaction between the spin of the metal and the spin of the π -radical cation can be tuned using the magnetic orbital topology by changing the metal and the connecting bridge as already done for metal complexes containing nitronyl nitroxide radical, for example.¹⁶ This compound is not conducting, but it clearly opens the way for the synthesis of new compounds by using other pyridine substituted TTF derivatives as ligands,¹⁷ and also by changing the transition metal and the counteranion, and crystal engineering. Without doubt, conducting and magnetic π -d systems and other properties might be achieved in the near future using this kind of coordination complex.

The solvents were distilled before use, and the starting reagents were used as received. TTF-py¹⁸ was synthesized as described in the literature. The monosubstituted $\text{Cu}(\text{hfac})_2(\text{TTF-py})$ was synthesized in the same way as the bis-substituted analogue¹⁰ using less than 2 equiv of TTF-py ligand for 1 equiv of the $\text{Cu}(\text{hfac})_2 \cdot \text{H}_2\text{O}$ unit. Black plate crystals were obtained by galvanostatic ($I = 5 \mu\text{A}$) oxidation of $\text{Cu}(\text{hfac})_2(\text{TTF-py})$ (10 mg) under argon atmosphere, using $(\text{Bu}_4\text{N})[\text{PF}_6]$ (100 mg) in CH_2Cl_2 (20 mL) as electrolytes. The stoichiometry of target material was determined from X-ray crystal structure analysis.

The crystallographic data have been deposited with the Cambridge Crystallographic Data Center as supplementary publication CCDC-190472. (Copies of the data can be obtained free of charge on application to CCDC, 12 Union Road, Cambridge CB21EZ, U.K. Fax: (+44)1223-336-033. E-mail: deposit@ccdc.cam.ac.uk.)

Acknowledgment. Financial support from CNRS (PICS program No 1433), Université de Rennes 1, and NEDO research project 00MB4

Supporting Information Available: Crystallographic information in CIF format. This material is available free of charge via the Internet at <http://pubs.acs.org>.

IC026211H

- (16) (a) Caneschi, A.; Ferraro, F.; Gatteschi, D.; Rey, P.; Sessoli, R. *Inorg. Chem.* **1990**, *29*, 4217. (b) Ouahab, L.; Dasna, I.; Golhen, S.; Daro, N.; Sutter, J.-P. In *Molecular Low Dimensional and Nanostructured Materials for Advanced Applications*; Graja, A., Bulka, B. R., Kajzar, F., Eds.; NATO ASI series; Kluwer Academic Publishers: Norwell, MA, 2002; pp 201–208.
- (17) (a) Liu, S.-X.; Dolder, S.; Pilkington M.; Decurtins, S. *J. Org. Chem.* **2002**, *67* (9), 3160. (b) Xu, W.; Zhang, D.; Li, H.; Zhu, D. *J. Mater. Chem.* **1999**, *9*, 1245.
- (18) Andreu, R.; Malfant, I.; Lacroix, P.G.; Cassoux, P. *Eur. J. Org. Chem.* **2000**, 737.